CONFORMAL METHOD FOR THE RECTILINEAR DIGITAL WAVEGUIDE MESH

Jung Suk Lee, Gary P. Scavone and Philippe Depalle

Music Technology Area
Schulich School of Music, McGill University
CIRMMT
Montreal, QC, Canada
jungsuk.lee@mail.mcgill.ca, {gary, depalle}@music.mcgill.ca

Moonseok Kim

kim.moonseok@gmail.com

ABSTRACT

The digital waveguide mesh (DWM) has proven to an efficient and accurate method for simulating multi-dimensional wave propagation in various applications such as physical modeling of musical instruments and room acoustics. However, problems appear when fitting a DWM to an arbitrary boundary because of the geometric constraints of a given mesh element. A finer mesh grid is often used in an attempt to resolve this situation, which entails an associated computational cost increase. This paper presents a conformal method for the rectilinear DWM as an efficient alternative. The proposed conformal method aims at better approximating rigid boundaries that are normally not well suited for a rectilinear DWM structure. It is inspired by the conformal method developed for the Finite Domain Time Difference (FDTD) scheme where a cell associated with the boundary is split with respect to a particular criterion and the material constant of the cell is adjusted accordingly [1]. By means of the interleaved waveguide network (IWN) [2], the conformal method is successfully achieved in the DWM.

Index Terms— Digital waveguide mesh, Finite domain time difference scheme, conformal method, interleaved waveguide network.

1. INTRODUCTION

The digital waveguide mesh (DWM) is an extension of the one-dimensional digital waveguide to multiple dimensions, describing wave propagation by using the d'Alembert solution of the wave equation [3]. Due to its simple and intuitive structure, the DWM has been actively studied in the realms of physical modeling of musical instruments, room acoustics and speech processing [4]. However, due to its inherent geometrical limits, errors occur when dealing with boundary shapes that do not well fit a given mesh grid. Such an error may be alleviated by using a finer mesh grid or a more complex mesh structure, but such approaches result in higher computational complexities. In contrast, Laird *et al.*[5] proposed a novel approach that makes use of a triangular mesh structure attached with *rimguides*, which is a set of additional fractional delays, giving rise to a better fit to curved boundaries.

In this paper, we propose another way of efficiently dealing with boundaries that don't exactly fit a DWM grid. It is motivated by the conformal method developed for the Finite Domain Time Difference (FDTD) scheme, originally proposed in [6] addressing electromagnetic wave propagation. Schneider *et al.*[1]'s conformal method addressed the problem of simulating acoustic wave propagation using the FDTD involving a pressure-release boundary that

doesn't fit an FDTD grid. In a cell associated with a velocity node through which the boundary passes, the cell is split if a certain criterion is satisfied and then the mass associated with the cell is reduced by half. We extend this simple yet efficient method to the DWM using an interleaved waveguide network (IWN) [2], which gives access to a velocity node in a DWM in the form of a scattering junction.

The remainder of this paper is organized as follows. Section 2 provides a review of the conformal methods developed for the FDTD. In Section 3, we present a conformal method for the DWM using the IWN, and Section 4 presents the simulation result of the conformal method in the DWM as well as a comparison against the FDTD simulation.

2. CONFORMAL METHOD IN FDTD

2.1. Staircase approximation

In the 2D FDTD scheme, the simplest way of modeling the pressure-release region, referred to as the *Stair-p* method [1], is to set the pressure node outside the boundary to zero. This arises when $0 < L \leq 1$ in Figure 1 which illustrates a cell associated with a velocity node. Other nodes are updated according to the usual FDTD update equations [1]:

$$
\begin{aligned}
p_{i,j}(n) = \; & p_{i,j}(n-1) \\
& - \rho \frac{c^2 T}{\Delta}[v_{x,i+\frac{1}{2},j}(n-\tfrac{1}{2}) - v_{x,i-\frac{1}{2},j}(n-\tfrac{1}{2})] \\
& - \rho \frac{c^2 T}{\Delta}[v_{y,i,j+\frac{1}{2}}(n-\tfrac{1}{2}) - v_{y,i,j-\frac{1}{2}}(n-\tfrac{1}{2})]
\end{aligned}
\tag{1}
$$

$$
\begin{aligned}
v_{x,i+\frac{1}{2},j}(n+\tfrac{1}{2}) = \; & v_{x,i+\frac{1}{2},j}(n-\tfrac{1}{2}) \\
& - \frac{T}{\rho\Delta}(p_{i+1,j}(n) - p_{i,j}(n))
\end{aligned}
\tag{2}
$$

$$
\begin{aligned}
v_{y,i,j+\frac{1}{2}}(n+\tfrac{1}{2}) = \; & v_{y,i,j+\frac{1}{2}}(n-\tfrac{1}{2}) \\
& - \frac{T}{\rho\Delta}(p_{i,j+1}(n) - p_{i,j}(n))
\end{aligned}
\tag{3}
$$

where the value of pressure at time step n is denoted as $p(n)$ with the subscript (i,j), indicating the node location in the grid and the values of velocity are denoted as $v_x(n), v_y(n)$ for x and y components, subscripted in the same way as the pressure value. ρ and c are the mass density and the speed of wave propagation of the acoustic medium. Δ and T are the spatial step and the time step, respectively. Another staircase approximation method, referred to as the

Stair-v method [1], sets a pressure node to zero if any of its neighboring velocity nodes are outside the boundary, in order to avoid the large distortion that would occur if using *Stair-p* method when $0 < L < 1/2$ (Figure 1).
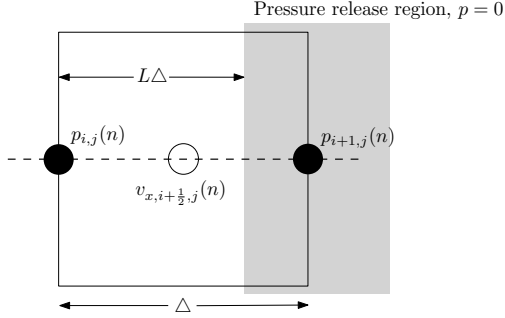

Figure 1: A 2D FDTD cell in which a velocity node $v_{x,i+\frac{1}{2},j}$ is centered.

2.2. Conformal method

In [1], authors proposed a simple conformal method in the FDTD scheme to handle a boundary that doesn't fit a FDTD grid. Their conformal method not only sets pressure nodes outside the boundary to zero but also takes into account the change of the mass in the cell as the cell at the boundary is split. From Figure 1, Newton's second law can be derived as

$$\rho\Delta^2 \frac{\partial}{\partial t} v_{x,\,i+\frac{1}{2},\,j} = -\Delta(p_{i+1,j} - p_{i,j}) \tag{4}$$

where the force difference between the left-side and the right-side of the cell is represented at the right-hand side. Under the assumption that a pressure-release boundary exactly passes through the center of the cell in Figure 1 in such a way that $L = 1/2$, then the mass of the cell is reduced by half, and from (4) we can derive the following equation by using the central difference scheme for the time derivative in the left-hand side.

$$v_{x,i+\frac{1}{2},j}(n+\tfrac{1}{2}) = v_{x,i+\frac{1}{2},j}(n-\tfrac{1}{2}) - \frac{2T}{\rho\Delta}(p_{i+1,j}(n) - p_{i,j}(n)) \tag{5}$$

The factor 2 on the right-hand side of (5) indicates the mass reduction by half and (5) can be viewed as a modified version of updating equation (2), to be assigned to a split-cell.

The authors of [1] also proposed a more advanced criterion of splitting a cell referred to as the *quantized split-cell* (QSC) method and showed that it yields more accurate results than those obtained when using either *Stair-p* or *Stair-v* method. Figure 2 shows the scenarios of splitting a cell containing either a v_x node or a v_y node using the QSC method. A cell is split when the two following conditions are satisfied : 1) the boundary line intersects the mid-line (the dashed-line in the middle that passes through all three nodes) of the cell and 2) the intersection is within the range of $1/4 < L < 3/4$, as shown in Figure 2, regardless of the curvature and the tilt of the boundary. Then, the pressure node outside the boundary is set to zero while the velocity node is updated according to the modified update equation (5). The authors of [1] also investigated reducing the mass of the cell by a factor of $1/L$, rather than 2, but found mixed results in terms of accuracy.
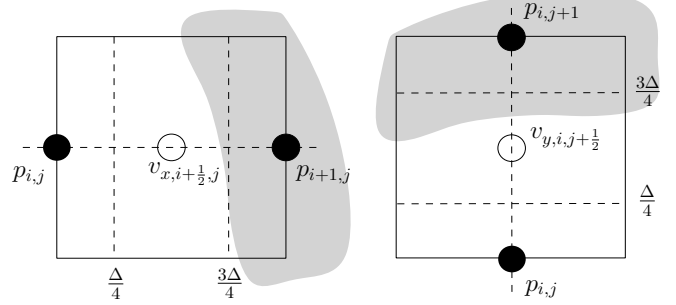

Figure 2: Split cells, Left : cell of v_x node, right : cell of v_y node. Grey region represents the pressure-release region.

## 3. CONFORMAL METHOD FOR THE RECTILINEAR DWM

Since the conformal method needs access to a velocity node placed in between the neighboring pressure nodes for cell-splitting and mass reduction, we employed an IWN to consider a velocity node in a rectilinear DWM where only pressure nodes are present in general. The IWN contains junctions of both pressure and velocity, placed a half sample apart in both x and y directions from each other, as in the FDTD scheme. In addition, by attaching a self-loop to a junction, spatially varying material constants (the mass density and the bulk modulus in the case of acoustic waves) can be handled. At the velocity node of the split cell in the FDTD scheme, the mass density is different from that inside the boundary by a factor of 0.5. To deal with the reduced mass at the split cell in a DWM, mass reduction should be considered at the velocity junction, and thus the voltage-centered type IWN [2] is used. The voltage-centered type IWN enables adjustment of the material constant at the velocity junction; therefore a reduction of mass in the velocity node can be managed in a way analogous to the conformal method in the FDTD scheme. In the voltage-centered type IWN, pressure junctions are updated using the general parallel junction update equation and a series velocity junction located between pressure junctions is updated in accordance with the update equation derived from the scattering junction relation. To derive the update equation for the velocity junction of a split cell, the scattering junction associated with a self-loop should first be investigated. As described in [1], for example, we consider a lossless acoustic medium and the situation given in the left side of Figure 2 where the boundary line is such that the condition for the QSC method is satisfied. By means of the voltage-centered type IWN, impedances of the velocity junction at the $(i+\frac{1}{2}, j)$ are given as [2],

$$Z_{W,i+\frac{1}{2},j} = \frac{1}{Y_{E,i,j}} = v_0\rho_{i,j} \tag{6}$$

$$Z_{E,i+\frac{1}{2},j} = \frac{1}{Y_{W,i+1,j}} = v_0\rho_{i+1,j} \tag{7}$$

$$Z_{C,i+\frac{1}{2},j} = v_0\frac{(\rho_{i,j} + \rho_{i+1,j})}{2} - v_0(\rho_{i,j} + \rho_{i+1,j}) \tag{8}$$

where $Y_{E,i,j}$, $Y_{W,i+1,j}$ are the east side and west side port admittances of the pressure junctions at the nodes (i,j) and $(i+1,j)$, respectively. We use N, S, E, W, C respectively indicating north, south, east, west and the self-loop for the notation of directions hereafter. $Z_{W,i+\frac{1}{2},j}, Z_{E,i+\frac{1}{2},j}$ and $Z_{C,i+\frac{1}{2},j}$ are the west side, the
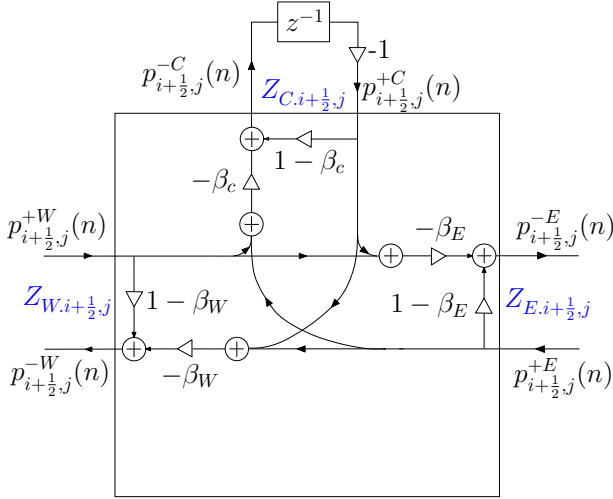
Figure 3: Scattering relation at the velocity junction $(i + \frac{1}{2}, j)$

east side and the self-loop port impedances of the velocity junction at the node $(i + \frac{1}{2}, j)$, respectively. $\rho_{i,j}$, $\rho_{i+1,j}$ are the mass densities at the nodes (i, j) and $(i+1, j)$, respectively and v_0 is defined as the ratio $\frac{\Delta}{T}$. We let $\rho_{i,j} = \rho_{i+1,j}$ to preserve the relation $v_0 = \sqrt{2}c$ [7] for the 2D DWM at all nodes, satisfying the Courant-Friedrichs-Lewy (CFL) condition. Note that the factor 2 in the denominator of the first term on the right-hand side of (8) indicates that the mass is reduced to half, corresponding to the factor 2 in (5), and the second term on the right-hand side of (8) is described in terms of the mass density, by converting the bulk modulus to the mass density using the relation $c = \sqrt{(bulk\ modulus)/(mass\ density)}$. By letting $\rho_{i,j} = \rho_{i+1,j} = \rho$, impedances above can be re-written as,

$$Z_{W,i+\frac{1}{2},j} = Z_{E,i+\frac{1}{2},j} = v_0\rho \qquad (9)$$
$$Z_{C,i+\frac{1}{2},j} = -v_0\rho \qquad (10)$$

As this scattering occurs at the series junction of velocity, we can derive scattering relations in terms of wave variables. Reflection and transmission coefficients characterizing the scattering junction can be obtained by first deriving *beta parameters* from the impedances in (9) and (10) [7] as follows

$$\beta_W = \frac{2Z_{W,i+\frac{1}{2},j}}{Z_{E,i+\frac{1}{2},j} + Z_{W,i+\frac{1}{2},j} + Z_{C,i+\frac{1}{2},j}} = 2 \qquad (11)$$

$$\beta_E = \frac{2Z_{E,i+\frac{1}{2},j}}{Z_{E,i+\frac{1}{2},j} + Z_{W,i+\frac{1}{2},j} + Z_{C,i+\frac{1}{2},j}} = 2 \qquad (12)$$

$$\beta_C = \frac{2Z_{C,i+\frac{1}{2},j}}{Z_{E,i+\frac{1}{2},j} + Z_{W,i+\frac{1}{2},j} + Z_{C,i+\frac{1}{2},j}} = -2. \qquad (13)$$

Thus expressions of pressure wave variables describing the series junction at $(i + \frac{1}{2}, j)$ are given as (Figure 3)

$$p_{i+\frac{1}{2},j}^{-W}(n) = (1 - \beta_W)p_{i+\frac{1}{2},j}^{+W}(n) - \beta_W(p_{i+\frac{1}{2},j}^{+E}(n) + p_{i+\frac{1}{2},j}^{+C}(n))$$
$$= -p_{i+\frac{1}{2},j}^{+W}(n) - 2(p_{i+\frac{1}{2},j}^{+E}(n) + p_{i+\frac{1}{2},j}^{+C}(n)) \qquad (14)$$

$$p_{i+\frac{1}{2},j}^{-E}(n) = (1 - \beta_E)p_{i+\frac{1}{2},j}^{+E}(n) - \beta_E(p_{i+\frac{1}{2},j}^{+W}(n) + p_{i+\frac{1}{2},j}^{+C}(n))$$
$$= -p_{i+\frac{1}{2},j}^{+E}(n) - 2(p_{i+\frac{1}{2},j}^{+W}(n) + p_{i+\frac{1}{2},j}^{+C}(n)) \qquad (15)$$

$$p_{i+\frac{1}{2},j}^{-C}(n) = (1 - \beta_C)p_{i+\frac{1}{2},j}^{+C}(n) - \beta_C(p_{i+\frac{1}{2},j}^{+E}(n) + p_{i+\frac{1}{2},j}^{+W}(n))$$
$$= 3p_{i+\frac{1}{2},j}^{+C}(n) + 2(p_{i+\frac{1}{2},j}^{+E}(n) + p_{i+\frac{1}{2},j}^{+W}(n)) \qquad (16)$$

The naming convention for a pressure wave variable $p_{i,j}^{-q}(n)$ is such that $+, -$ signs in the superscript mean 'incoming' to and 'outgoing' from the junction at the node (i, j), respectively and q in the superscript indicates the direction that a junction side faces and the self loop, either N, S, E, W and C. If we write equations above in terms of wave variables associated with the junctions at (i, j) and $(i + \frac{1}{2}, j)$, we have

$$p_{i,j}^{+E}(n + \tfrac{1}{2}) = -p_{i,j}^{-E}(n - \tfrac{1}{2}) - 2(p_{i+1,j}^{-W}(n - \tfrac{1}{2}) + p_{i+\frac{1}{2},j}^{-C}(n)) \qquad (17)$$

$$p_{i+1,j}^{+W}(n + \tfrac{1}{2}) = -p_{i+1,j}^{-W}(n - \tfrac{1}{2}) - 2(p_{i,j}^{-E}(n - \tfrac{1}{2}) + p_{i+\frac{1}{2},j}^{-C}(n)) \qquad (18)$$

$$p_{i+\frac{1}{2},j}^{-C}(n) = 3p_{i+\frac{1}{2},j}^{+C}(n) + 2(p_{i+1,j}^{-W}(n - \tfrac{1}{2}) + p_{i,j}^{-E}(n - \tfrac{1}{2})) \qquad (19)$$

By shifting half samples in all variables in (17), (18), we obtain

$$p_{i,j}^{+E}(n) = -p_{i,j}^{-E}(n - 1) - 2(p_{i+1,j}^{-W}(n - 1) + p_{i+\frac{1}{2},j}^{-C}(n - \tfrac{1}{2})) \qquad (20)$$

$$p_{i+1,j}^{+W}(n) = -p_{i+1,j}^{-W}(n - 1) - 2(p_{i,j}^{-E}(n - 1) + p_{i+\frac{1}{2},j}^{-C}(n - \tfrac{1}{2})) \qquad (21)$$

From the relation, $p_{i+\frac{1}{2},j}^{-C}(n - 1) = -p_{i+\frac{1}{2},j}^{+C}(n)$, we have:

$$p_{i+\frac{1}{2},j}^{-C}(n)$$
$$= -3p_{i+\frac{1}{2},j}^{-C}(n - 1) + 2(p_{i+1,j}^{-W}(n - \tfrac{1}{2}) + p_{i,j}^{-E}(n - \tfrac{1}{2})) \qquad (22)$$

Thus,

$$p_{i+\frac{1}{2},j}^{-C}(n - \tfrac{1}{2})$$
$$= -3p_{i+\frac{1}{2},j}^{-C}(n - \tfrac{3}{2}) + 2(p_{i+1,j}^{-W}(n - 1) + p_{i,j}^{-E}(n - 1)). \qquad (23)$$

By substituting (23) into (20) and (21), we can supply all the necessary wave variables to the neighboring pressure junctions $p_{i,j}$ and $p_{i+1,j}$ for the update in the DWM. $p_{i+\frac{1}{2},j}^{-C}(n)$ is the only variable to be determined to operate the scattering junction and we initially set this value as zero.

4. SIMULATION RESULT

We consider an ideal circular surface in the rectilinear 2D DWM with no loss, assuming a pressure-release region outside the boundary. Therefore, pressure traveling waves are perfectly reflected at the boundary. The mode frequencies of this ideal circular surface are given analytically as [8]:

$$f_{mn} = \frac{c}{2\pi r} x_{mn}. \qquad (24)$$

where r is the diameter of the circular membrane and x_{mn} is the
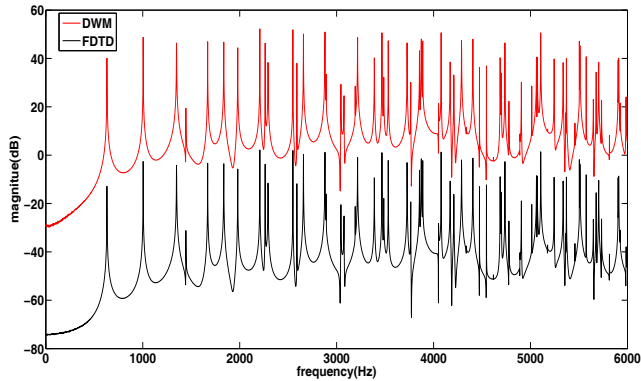

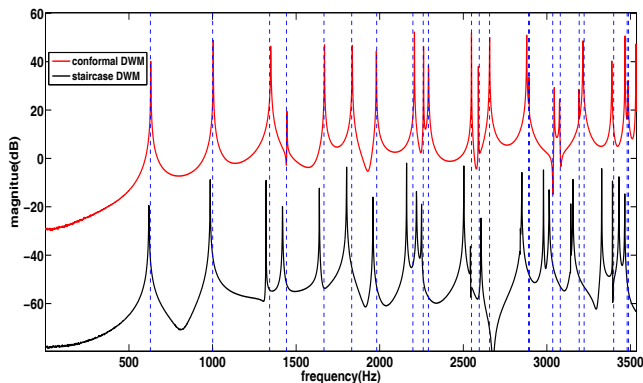Figure 4: Results of the conformal method, Top : DWM, Bottom : FDTD

Figure 5: The upper line is the magnitude response of the DWM simulation with the conformal method and the lower line is that of the DWM simulation with the *Stair-p* method. The blue dashed lines indicate the frequencies of the modes as given by (24).

nth zero crossing point of the Bessel function $J_m(x)$, respectively. In this simulation, the radius of the circle is set to 19 spatial samples (19Δ). The sampling rate used is 44100Hz. A gaussian pulse of width 4 ($\sigma = 4$ for $\frac{1}{\sigma\sqrt{2\pi}} e^{-\frac{x^2+y^2}{\sigma^2}}$) is injected at the center node ($(0,0)$) of the circle and the pressure value at the node (-6,6) is picked up. We first compared the FDTD simulation result and the DWM simulation result obtained from the conformal method to

verify that the results are the same. Figure 4 shows the comparison of these two results. Figure 5 shows the comparison between the DWM simulation with the *Stair-p* method and the one with the conformal method. It is shown that mode frequencies obtained using the conformal method are better aligned with the analytic solution up to 3500 Hz. At higher frequencies, however, the conformal method becomes increasingly subject to distortion, though always outperforming the *Stair-p* method. While the computational complexity at a split node is significantly higher than that of simple fixed- or open-boundary reflection, split nodes only exist along boundaries and thus, in general, this method will not significantly increase the computational demands of a complete simulation.

5. CONCLUSION

We presented a conformal method for the 2D DWM to efficiently manage the situation where a mesh grid does not fit the boundaries of a given shape. Using an IWN, a scattering junction at the velocity node of a split cell is constructed, enabling the adjustment of the mass of the cell. The proposed conformal method in a DWM shows the same results as the one obtained using the conformal method originally developed for the 2D FDTD scheme. Accordingly, the proposed conformal method improves the performance of a DWM model when dealing with the boundary as described. Future work includes extensions to higher dimension DWMs and other types of boundary condition besides the rigid boundary.

6. REFERENCES

[1] J. B. Schneider, C. L. Wagner and R. J. Kruhlak, "Simple conformal methods for finite-difference time-domain modeling of pressure-release surfaces," *J. Acoust. Soc. Am.* vol. 104, no. 6, pp. 3219-3226, December 1998.

[2] S. Bilbao, *Wave and scattering methods for the numerical integration of partial differential equations.* John and Wiley, 2004.

[3] S. A. V. Duyne and J. O. Smith, "Physical modeling with the 2-D digital waveguide mesh," in *Proc. Int. Computer Music Conference (ICMC)*, Tokyo, Japan, September 1993, pp. 40-47.

[4] D. T. Murphy, A. Kelloniemi, J. Mullen and S. Shelley, "Acoustic modeling using the digital waveguide mesh," *IEEE Signal Processing Magazine*, vol. 24, no. 2, pp 55-66, March 2007.

[5] J. Laird, P. Masri and N. Canagarajah, "Efficient and accurate synthesis of circular membranes using digital waveguides," In *IEE Colloqium : Audio and Music Technology : The Challenge of Creative DSP*, 1998.

[6] S. Dey and R. Mittra, "A locally conformal finite-difference time-domain (FDTD) algorithm for modeling three-dimensional perfectly conducting objects," *IEEE Microwave and Guid. Wave Lett.* vol. 7, no. 9, pp. 273-275, 1995.

[7] J. O. Smith, *Physical Audio Signal Processing.* December 2009, online book.

[8] P. M. Morse, *Vibration and Sound.* American Institute of Physics for the Acoustical Society, 1981.